Submitted manuscript entitled: Danger of groundwater contamination widely underestimated because of shortcuts for aquifer recharge

Submitted to: Nature Sustainability on April 23rd 2020

Authors: Andreas Hartmann[1,2*], Scott Jasechko[3], Tom Gleeson[4], Yoshihide Wada[5,6], Bartolomé Andreo[7], Juan Antonio Barberá[7], Heike Brielmann[8], Lhoussaine Bouchaou[9,10], Jean-Baptiste Charlier[11], W George Darling[12], Maria Filippini[13], Jakob Garvelmann[14,15], Nico Goldscheider[16], Martin Kralik[17], Harald Kunstmann[14,18], Bernard Ladouche[11], Jens Lange[19], Giorgia Lucianetti[20], José Francisco Martín[7], Matías Mudarra[7], Damián Sanchez[7], Christine Stumpp[21], Eleni Zagana[22], Thorsten Wagener[2,23]

Author affiliations:
[1] Chair of Hydrological Modeling and Water Resources, University of Freiburg, Germany
[2] Department of Civil Engineering, University of Bristol, United Kingdom
[3] Bren School of Environmental Science and Management, Univ. Calif. Santa Barbara, Santa Barbara, CA, 93117, USA
[4] Department of Civil Engineering and School of Earth and Ocean Sciences, University of Victoria, Canada
[5] International Institute for Applied Systems Analysis, Schlossplatz 1, A-2361, Laxenburg, Austria
[6] Department of Physical Geography, Utrecht University, Utrecht, The Netherlands, Heidelberglaan 2, 3584 CS Utrecht, The Netherlands
[7] Department of Geology and Centre of Hydrogeology at the University of Malaga (CEHIUMA), Malaga, Spain
[8] Austrian Federal Environmental Agency, Vienna, Austria
[9] Laboratory of Applied Geology and Geo- Environment, Ibn Zohr University, Agadir, Morocco
[10] Mohammed VI Polytechnic University, International Water Research Institute, Morocco
[11] BRGM, Univ. Montpellier, Montpellier, France
[12] British Geological Survey, Wallingford, United Kingdom
[13] Department of Biological Geological and Environmental Sciences, Alma Mater Studiorum - University of Bologna, Italy
[14] Institute of Meteorology and Climate Research, Karlsruhe Institute of Technology, Campus Alpin, Garmisch-Partenkirchen, Germany
[15] boden & grundwasser~ Allgäu GmbH, Sonthofen, Germany
[16] Institute of Applied Geosciences, Karlsruhe Institute of Technology (KIT), Karlsruhe, Germany
[17] Department of Environmental Geosciences, University of Vienna, Austria
[18] Institute of Geography, University of Augsburg, Augsburg, Germany
[19] Chair of Hydrology, University of Freiburg, Germany
[20] Department of Sciences, Roma Tre University, Largo S. Leonardo Murialdo 1, 00146 Rome, Italy
[21] University of Natural Resources and Life Sciences, Institute for Soil Physics and Rural Water Management, Muthgasse 18, 1190, Vienna, Austria
[22] Laboratory of Hydrogeology, Department of Geology, University of Patras, 26500 Rion Patras, Greece
[23] Cabot Institute, University of Bristol, United Kingdom

Corresponding author:
Andreas Hartmann
Chair of Hydrological Modeling and Water Resources
University of Freiburg
Friedrichstrasse 39, 79098 Freiburg, Germany
Tel.: 0049.761.203.3520 | Fax: 0049.761.203.3594
andreas.hartmann@hydmod.uni-freiburg.de

Words (abstract): 150
Words (main text): 2117
Words (methods): 1160
Number of figures: 3
References: 40

Main text

Groundwater pollution threatens human and ecosystem health in many areas around the globe. Shortcuts to the groundwater through concentrated recharge are known to transmit short-lived pollutants into carbonate aquifers endangering water quality of around a quarter of the world population. However, the large-scale impact of such concentrated recharge on water quality remains poorly understood. Here we apply a continental-scale model to quantify the danger of groundwater contamination by degradable pollutants through concentrated recharge in carbonate rock regions. We show that in regions where concentrated recharge takes place, the percentage of non-degraded pollutants in groundwater recharge increases from <1% to around 10-50%. In those regions, pollutants like Glyphosate can exceed their permissible concentrations by up to 19 times when reasonable application rates are assumed. Our results imply that in times of continuing industrial agricultural productivity, shortcuts to the groundwater may result in a widespread and substantial reduction of usable groundwater volumes.

Clean water is essential for nature and society[1] but pollution may result in a widespread reduction of available drinking water and in a threat to ecosystem services[2]. Large-scale studies on water security so far have mainly focused on water quantity rather than water quality[3]. Local studies have shown that concentrated recharge is a dominant driver for the pollution of groundwater resources in carbonate rock regions[4,5]. Fast flow through fractures and macropores in the soil can substantially mobilize pollutants even though some have been considered 'non-leachable' owing to their strong adsorption to colloids and sediment surfaces in the soil or due to fast degradation times[6]. Consequently, in addition to the dangers of more persistent pollutants like nitrate[7], concentrated recharge may cause unexpected groundwater quality deterioration in regions where agriculture relies on degradable fertilizers and pesticides[8,9]. Although agriculture occupies around 40% of ice-free lands[10], as of yet there are no continental-scale assessments of the impact of concentrated recharge and degradable pollutants on groundwater quality.

This work estimates the danger of groundwater contamination via shortcuts for recharge to the groundwater by enlarged cracks and fissures, often referred to as concentrated recharge[11]. We do this by contrasting the travel times of water from the surface to the subsurface with the degradation times of typical agricultural pollutants. Our research domain is the carbonate rock regions of Europe, Northern Africa and the Middle East, collectively home to around half a billion people and provider of up to half of national water supplies in these regions[12]. Globally,

10-25% of the world population are estimated to largely or entirely depend on groundwater from carbonate rock aquifers[13,14]. Chemical weathering (in this context often referred to as karstification) increases the abundance of concentrated recharge, resulting in shortcuts between the surface and the subsurface[15]. During rainfall events, this characteristic of karstified carbonate rock allows large volumes of water to enter the subsurface[12,16] and can transport surface-borne pollutants – dissolved or attached to suspended sediments – to the groundwater at short time scales, i.e. within days or weeks[17,18]. We derive the fractions of groundwater recharge that correspond to these short time scales, here referred to as *rapid recharge fractions*, by simulating transit time distributions with a state-of-the-art continental model [16] that accounts for concentrated recharge processes in carbonate rock regions. For analysis, our simulation domain is divided into four regions: humid, mountains, Mediterranean, and deserts (see model description in methods section).

Continental-scale estimation of rapid recharge fractions

We derive the rapid recharge fractions using the half-life times and survival times of three example pollutants, veterinary pharmaceuticals in manure (Salinomycin, 10-day half-life time[8]), degradable pesticides (Glyphosate, 25-day half-life time[19]), and pathogens (E. coli, 60-day survival time[9]). We limit our simulated rapid recharge times of pollutant transfer to the groundwater to 5 days as immediate transfer after rainfall events, and to 90 days as transfer within the same season. We quantify the influence of concentrated recharge processes on fast transit to the groundwater by repeating the same procedure with concentrated recharge turned off in our model (see model description in methods section). That way, only diffuse recharge is simulated similarly to presently available large-scale hydrological models[12]. To explore the impact of climate, we compare simulated rapid recharge fractions with climate descriptors such as mean annual precipitation and temperature, aridity index (defined as long-term ratio of precipitation to potential evapotranspiration), mean annual number of rainfall events, and mean annual duration of snow cover. We evaluate the consistency of our model with independently derived Young Water Fractions – the fraction of water less than 60-90 days old[20,21] - corrected for precipitation seasonality[22] at 119 carbonate rock springs across our simulation domain (see simulation of transit times in methods section) and with a dataset of >2,500 groundwater samples that were analysed for glyphosate abundance and concentration inside and outside the karst regions of the United States[23,24].

Our simulations indicate that in the Mediterranean, up to 77±14% of concentrated recharge transits to the groundwater within one season (90 days, Fig. 1a); in the mountain regions 50±17%, in the desert regions 46±11%, and in the humid regions 41±11%. Our comparison of the simulated rapid recharge fractions with the observed Young Water Fractions from the carbonate rock springs shows significant correlation ($r=0.83$, $p\leq0.001$). Though with some tendency to over-estimate observed Young Water Fractions for some springs in humid and mountain regions where observed Young Water Fractions are low. Using a 60-day threshold, this over-estimation reduces and is replaced by an under-estimation of high observed Young Water Fractions in the Mediterranean region ($r=0.79$, $p\leq0.001$, Fig. S3). The overall high correlation indicates realistic model behaviour and shows that of the 60-90 days old Young Water Fractions of the carbonate rock springs are most precisely simulated using the 90-day threshold for high rapid recharge fractions, while the 60-day threshold provides better estimates for lower rapid recharge fractions.

[Fig. 1 about here]

Factors controlling rapid transit to the groundwater

Concentrated recharge is the most important driver for the rapid transit of water from the land surface to groundwater. We use our simulation model to quantify the impact of concentrated recharge and climate on the abundance and strength of rapid transport of pollutants to the groundwater. When not considering concentrated recharge in our model, we find substantially reduced rapid recharge fractions (Mediterranean: 1±2%, mountain: 4±9%, desert: 0±0.2%, humid: 0±0.7% of rapid recharge compared to total recharge), indicating that concentrated recharge is the dominant mechanism for rapid transit to groundwater (Fig. 2). Including concentrated recharge, we find that rapid recharge fractions most strongly correlate with the aridity index for both Mediterranean and desert regions. The second strongest correlation is between the rapid recharge fractions and the average number of rainfall events per year as well as mean annual precipitation, both closely correlated with the aridity index ($r=0.65$ and $r=0.94$, both $p\leq0.001$, for the Mediterranean and desert regions, respectively). In humid and mountain regions, we find weaker yet still significant correlations of rapid recharge fractions with mean annual temperature and average months with snow cover ($0.44 \leq r \leq 0.51$ and $-0.3\,9\leq r \leq -0.35$, respectively).

[Fig. 2 about here]

Our simulations indicate that wetness, expressed by increasing values of the aridity index, mean annual precipitation, and mean annual number of rainfall events, are important secondary controls for the strength of rapid recharge fractions in the carbonate rock areas of the Mediterranean and the desert regions. This agrees with local studies already showed that limited soil storage capacities[25] and the formation of desiccation cracks and stormy periods favour the fast transit of water to the subsurface[26,27]. Although weak, the positive correlation with temperature and with the average number of snow months for the humid and mountain regions indicate a reduction of fast recharge through snow storage that may cause a longer delay to the precipitation signal until transmitted to the hydrological system[28]. Similar results are obtained when using the 60-day threshold to define the rapid recharge fractions (Fig. S5 and Fig. S6).

Quantification of the danger of groundwater contamination

Shortcuts into the groundwater increase the danger of groundwater contamination from pollutants of varying half-life times and survival times, particularly in the Mediterranean region. Our model calculates the rapid recharge fractions corresponding to varying pollutants with thresholds from 5 to 90 days (Fig. 3). In order to quantify the influence of concentrated recharge, we repeat the same procedure without considering concentrated recharge (see model description in methods section). We find that among the four regions rapid recharge fractions increase from 5.1-15.2% for the 5-day-threshold to 36.3-77.3% for the 90-day-threshold with the lowest rapid recharge fraction constantly found in the humid region, while the largest rapid recharge fractions are always produced by the Mediterranean regions. Averaging over all threshold times, concentrated recharge increases the rapid recharge fractions by 20.4±10.8% (humid region), 24.7±12.7% (mountain region), 27.7±10.9% (desert region), and 49.5±20.5% (Mediterranean), compared to averages of 0.01–0.76% when concentrated recharge is not considered (Fig. 3). Regarding our three example pollutants, we find that 9.9±8.8% of Salinomycin, 15.5±13.0% of Glyphosate, and 33.1%±21.5% of *E. coli* remain in groundwater recharge over all simulated carbonate regions when concentrated recharge is considered (Fig. 3). All three example pollutants show their largest rapid recharge fractions in the Mediterranean region where thin soils favour rapid fast transit of pollutants to the groundwater.

[Fig. 3 about here]

Using a realistic estimate of 175 mm a^{-1} recharge over our entire simulation domain[16], realistic Glyphosate application rates for wheat control of 0.72-4.32 kg ha^{-1} a^{-1} [29], and 50% degradation due to its half-life time of 25 days[19], mean concentrations of 0.32±0.27 µg l^{-1} to 1.91±1.61 µg l^{-1}

would still reach groundwater. These simulations exceed the maximum permissible concentration of single pesticides (0.1 µg l^{-1} [30]) 3.2–19.1 times, disregarding metabolites[31]. Although no comprehensive datasets exist in Europe to evaluate these modelled values, our results correspond well with a national survey conducted in the contiguous United States[23,24] that found concentrations of 1.82±1.74 µg l^{-1} in 93 glyphosate detections out of 751 groundwater samples collected from carbonate aquifers (Fig. S 7). Glyphosate was detected ~5.3 times more often within carbonate rock regions, and with concentrations ~4.1 times higher compared to non-carbonate rocks regions (0.45±0.66 µg l^{-1} in 42 detections out of 1805 groundwater samples), which supports our finding that concentrated recharge increases the danger of groundwater contamination at larger scales (Fig. 3).

Implications of potentially underestimated contamination

Our carbonate rock recharge estimates only consider vertical infiltration and percolation fluxes. We are aware that infiltrating pollutants may still experience attenuation in transit to the water supply system due to: (1) long travel times, as well as dispersion and diffusion processes, especially towards deep groundwater systems (our model accounts for depths up to ~30 m), (2) mixing with infiltrating waters from non-agricultural areas from which no contaminants originate, (3) mixing with less polluted groundwater that was recharged before application of the pollutant, (4) sorption to immobile colloids or sediment surfaces in the soil, or (5) removal or retardation of the pollutant during lateral groundwater flow towards a well. While toxicity disappears for most pathogens and pharmaceuticals after removal[8,9], pesticides can transform into metabolites that can be toxic[31]. Furthermore, the half-life times or survival times of all pollutants may strongly vary depending on moisture, temperature, and redox conditions in the unsaturated zone. For all these reasons, and despite their good agreement with observed Young Water Fractions and Glyphosate concentrations, our results should be seen as a first-order estimate and worst-case scenario of the potential danger of contamination through degradable pollutants in regions with significant subsurface heterogeneity.

Overall, our continental study clearly elaborates that the danger of contamination through concentrated recharge is not limited to individual sites but relevant across a larger scales. Especially in regions like the Mediterranean, travel times of recharge to the subsurface can be short, and decrease with increasing degree of aridity. In these regions the fast transit of agricultural pollutants to the groundwater poses a significant challenge for water and land use management. Rising human population and the increased consumption of water, food and

energy will increase pressure on agriculture and natural resources[10,32]. While carbonate rock regions can be a valuable source of drinking water[12], our results show that increasing agricultural production with the help of synthetic chemical fertilizers, pesticides and/or veterinary pharmaceuticals may cause substantial and pervasive groundwater pollution. This can result in a widespread reduction of available drinking water quality and harm ecosystem services more intensely than previously available large-scale models. While local approaches exist to map and protect areas with increased concentrated recharge[4], large-scale water quality models are urgently needed to identify regions of increased danger of drinking water contamination over large scales relevant for water governance[3]. Our approach is the first to quantify the danger of groundwater contamination over an entire continent and therefore supports water governance to ensure future water security and ecosystem services.

Methods

The carbonate rock recharge model

The model was developed to simulate carbonate rock groundwater recharge over Europe, Northern Africa and the Middle East (VarKarst-R[12,16]). It simulates terrestrial hydrological processes on a 0.25° x 0.25° grid and at a daily temporal resolution for a 10-year period from 2002 to 2012. Its conceptualization is derived from previous applications at the aquifer scale where high observation densities allowed thorough evaluation[33,34]. It includes the spatiotemporal variability of carbonate rock infiltration due to rainfall and snowmelt, evapotranspiration, downward percolation from the upper soil layer to a lower soil epikarst layer and vertical percolation from the epikarst layer towards the groundwater. The latter corresponds to depths up to ~30 m[33], considered in this study as the definitional groundwater depth to which recharge is added. Previous work shows that the model's representation of concentrated recharge provides more realistic estimates of groundwater recharge in carbonate rock regions compared to other large-scale hydrological models[12,16] because it assumes that even within the same hydrological landscape type there is a distribution of subsurface properties. This variability is considered through distribution functions that allow for variable subsurface storage capacities, as well as of vertical hydraulic properties, over *N* horizontally parallel model compartments:

$$S_{\max,i} = S_{\max,N}\left(\frac{i}{N}\right)^{a} \quad (1)$$

$$K_i = K_1\left(\frac{N-i+1}{N}\right)^{a} \quad (2)$$

where $S_{max,i}$ [mm] is the subsurface storage capacity of model compartment *i*, $S_{max,N}$ [mm] is the overall maximum subsurface storage capacity, K_i [d] describes the vertical hydraulic conductivity of the subsurface storage at model compartment *i*, K_1 [d] is the subsurface storage constant at model compartment 1, and *a* [-] is a dimensionless shape factor.

The model simulates *N* time series representing a range of spatially variable recharge dynamics: (a) slow and diffuse recharge at the model compartments with low hydraulic conductivities, (b) fast and concentrated recharge at those compartments with higher hydraulic conductivity, and (c) lateral redistribution of water from compartments with low hydraulic conductivity to compartments with higher hydraulic conductivity. When turning off concentrated recharge (Figure 2 and Figure 3), (b) and (c) are deactivated, which simulates diffuse recharge only producing similar groundwater recharge simulations as presently available large-scale hydrology models (e.g. PCR_GLOBWB[35] , see[12]).

Within our simulation domain, the model parameters were estimated for four regions, namely humid (HUM), mountains (MTN), Mediterranean (MED), and deserts (DES), which were identified by climatic and topographic information[16]. A large sample of initial model parameter sets (n=25,000) was created that was iteratively reduced using prior information (e.g.,FAO[25]), latent heat flux observations[36] and soil moisture observations[37] for the different regions. The remaining model parameter sets represent the remaining uncertainty of recharge simulations. Their absolute values indicate decreasing soil storages from the HUM and MTN regions toward the MED and DES regions[16].

Simulation of transit times to the groundwater

In order to estimate the simulated rapid recharge fractions corresponding to the half-life times and survival times of different pollutants, we first derived simulated transit time distributions from the model's groundwater recharge simulations using virtual tracer experiments. Each hydrological year of our simulations, a virtual tracer is applied to each grid cell's precipitation. Evaluation of the model with observed artificial tracer breakthrough curves[38] and transit times[39] at the catchment scale demonstrates that its representation of transport by mixing assumptions within all its variable compartments provides a realistic approximation of advection and dispersion processes in carbonate rock systems. The time when the simulated recharge reaches 50% of the input concentration of the tracer is assumed to approximate the mean transit time. By doing so for *N* simulated recharge time series (see above), a distribution of mean transit times can be derived. Using the evaluated transit time distribution, we can define threshold

times that correspond to the half-life times and survival times of selected pollutants and derive the corresponding fraction of simulated groundwater recharge, i.e. the concentrated fraction of groundwater recharge that still contains the selected pollutants.

To benchmark the simulated transit time distributions, we use 119 time series of observed water isotope dynamics of carbonate rock springs that we collected over the humid, Mediterranean, mountain and desert regions. As shown by preceding research[20,21], we can use the ratio of seasonal amplitudes of the water isotope composition of precipitation and spring discharge to estimate the Young Water Fraction (less than 60–90 days old). The amplitude of precipitation isotopic compositions is obtained from[40] while the amplitude of the carbonate rock springs is derived by fitting sine functions to the observed isotopic composition at the 119 carbonate rock springs. For realistic estimates, we (1) do not allow Young Water Fractions <0% and >100%, (2) discard those with a coefficient of determination of fitted sine curve and observations ≤ 0, and (3) remove those with more than 2 months of continuous snow cover, creating substantial delay before infiltration.

A preliminary comparison of observed Young Water Fractions of the non-discarded springs (78 in total, see Table S 3 and Table S 4) with the simulated rapid recharge fractions that are younger than 90 days (derived from the simulated transit time distributions) shows that the observed Young water fractions have to be corrected for seasonality of rainfall, which is already known to produce bias in Young Water Fraction estimation[22]. In our dataset, this bias is expressed as a strong correlation of rainfall seasonality (ratio of average precipitation in July, August and September and average precipitation in January, February and March) with the deviation between simulated rapid recharge fractions and observed Young Water Fractions (Fig. S 1). We use this correlation to obtain seasonality corrected estimates of observed Young Water Fractions (Fig. 1b). Uncertainty of the observed Young Water Fractions is expressed by the combined standard errors of the amplitude estimates of the rainfall and carbonate rock spring isotopic signals derived by Gaussian error propagation. Uncertainty of the simulated rapid recharge fractions represents the remaining uncertainty after parameter estimation of the continental recharge model (see above). Since the observed Young Water Fractions are only defined within a range (60–90 days), we repeat the same procedure with a 60-day threshold (see Fig. S 2 and Fig. S 3b).

Derivation of climatic controls

To explore the impact of climate on rapid recharge fractions, we derive different climate descriptors from the daily 10-year input data of the continental carbonate rock recharge model[16]: mean annual precipitation, mean annual temperature, aridity index (defined as mean annual precipitation over potential evapotranspiration), mean annual number of rainfall events, mean annual number of months with snow cover, high intensity rainfall events defined by the mean intensity of the upper quartile of rainfall events. We explore the linkage between these climatic controls and rapid recharge fractions using the seasonal threshold (90 days) because the model evaluation was performed using the same threshold (Table S1, Fig. 2 and Fig. S 4). The same procedure is repeated using the alternate threshold for the model evolution (60-day threshold, see Table S2, Fig. S 5 and Fig. S 6). Correlations are quantified through their Pearson correlation coefficients r and their significance p (using a significance level alpha of 0.05).

References

1. Hofstra, N., Kroeze, C., Flörke, M. & van Vliet, M. T. Editorial overview: Water quality: A new challenge for global scale model development and application. *Curr. Opin. Environ. Sustain.* **36**, A1–A5 (2019).

2. Hoekstra, A. Y. & Mekonnen, M. M. The water footprint of humanity. *Proc. Natl. Acad. Sci. U. S. A.* **109**, 3232–3237 (2012).

3. Van Vliet, M. T. H., Florke, M. & Wada, Y. Quality matters for water scarcity. *Nat. Geosci.* **10**, 800–802 (2017).

4. Daly, D. *et al.* Main concepts of the 'European approach' to karst-groundwater-vulnerability assessment and mapping. *Hydrogeol. J.* **10**, 340–345 (2002).

5. Andreo, B. *et al.* Karst groundwater protection: First application of a Pan-European Approach to vulnerability, hazard and risk mapping in the Sierra de Líbar (Southern Spain). *Sci. Total Environ.* **357**, 54–73 (2006).

6. Jarvis, N. J. A review of non-equilibrium water flow and solute transport in soil macropores: Principles, controlling factors and consequences for water quality. *Eur. J. Soil Sci.* **58**, 523–546 (2007).

7. Ascott, M. J. *et al.* Global patterns of nitrate storage in the vadose zone. *Nat. Commun.* **8**, 1–6 (2017).

8. Kümmerer, K. *Pharmaceuticals in the environment: sources, fate, effects and risks*.

(Springer Science & Business Media, 2008).

9. WHO. *Protecting groundwater for health: managing the quality of drinking-water sources*. (World Health Organization, 2006).

10. Foley, J. A. *et al.* Solutions for a cultivated planet. *Nature* **478**, 337–342 (2011).

11. de Vries, J. J. & Simmers, I. Groundwater recharge: An overview of process and challenges. *Hydrogeol. J.* **10**, 5–17 (2002).

12. Hartmann, A., Gleeson, T., Wada, Y. & Wagener, T. Enhanced groundwater recharge rates and altered recharge sensitivity to climate variability through subsurface heterogeneity. *Proc. Natl. Acad. Sci. U. S. A.* **114**, 2842–2847 (2017).

13. Stevanović, Z. Karst waters in potable water supply: a global scale overview. *Environ. Earth Sci.* **78**, 1–12 (2019).

14. Chen, Z. *et al.* The World Karst Aquifer Mapping project: concept, mapping procedure and map of Europe. *Hydrogeol. J.* (2017). doi:10.1007/s10040-016-1519-3

15. Worthington, S. R. H., Davies, G. J. & Alexander, E. C. Enhancement of bedrock permeability by weathering. *Earth-Science Rev.* **160**, 188–202 (2016).

16. Hartmann, A. *et al.* A large-scale simulation model to assess karstic groundwater recharge over Europe and the Mediterranean. *Geosci. Model Dev.* **8**, (2015).

17. White, W. B. *et al. Karst groundwater contamination and public health*. (Springer, 2016). doi:10.1007/978-3-319-51070-5

18. Bridget R. Scanlon, Richard W. Healy & Peter G. Cook. Choosing appropriate techniques for quantifying groundwater recharge. *Hydrogeol. J.* **10**, 18–39 (2002).

19. Lewis, K. A. *et al.* Human and Ecological Risk Assessment : An International An international database for pesticide risk assessments and management and management. *Hum. Ecol. Risk Assess.* **22**, 1050–1064 (2016).

20. Kirchner, J. W. Aggregation in environmental systems-Part 1: Seasonal tracer cycles quantify young water fractions, but not mean transit times, in spatially heterogeneous catchments. *Hydrol. Earth Syst. Sci.* **20**, 279–297 (2016).

21. Jasechko, S., Kirchner, J. W., Welker, J. M. & McDonnell, J. J. Substantial proportion of global streamflow less than three months old. *Nat. Geosci.* **9**, 126–129 (2016).

22. Kirchner, J. W. Aggregation in environmental systems-Part 2: Catchment mean transit times and young water fractions under hydrologic nonstationarity. *Hydrol. Earth Syst. Sci.* **20**, 299–328 (2016).

23. Scribner, E. A., Battaglin, W. A., Gilliom, R. J. & Meyer, M. T. Concentrations of Glyphosate, Its Degradation Product, Aminomethylphosphonic Acid, and Glufosinate in Ground- and Surface-Water, Rainfall, and Soil Samples Collected in the United States, 2001–06. *U.S. Geol. Surv. Sci. Investig. Rep.* **2007**–**5122**, (2007).

24. Read, E. K. *et al.* Water quality data for national-scale aquatic research: The Water Quality Portal. *Water Resour. Res.* **53**, 1735–1745 (2017).

25. FAO. *Digital Soil Map of the World*. (2003).

26. Martínez-Murillo, J. F., Nadal-Romero, E., Regüés, D., Cerdà, A. & Poesen, J. Soil erosion and hydrology of the western Mediterranean badlands throughout rainfall simulation experiments: A review. *Catena* **106**, 101–112 (2013).

27. Andreo, B. *et al.* Influence of rainfall quantity on the isotopic composition (18O and 2H) of water in mountainous areas. Application for groundwater research in the Yunquera-Nieves karst aquifers (S Spain). *Appl. Geochemistry* **19**, 561–574 (2004).

28. Paul Stockinger, M., Reemt Bogena, H., Lücke, A., Stumpp, C. & Vereecken, H. Time variability and uncertainty in the fraction of young water in a small headwater catchment. *Hydrol. Earth Syst. Sci.* **23**, 4333–4347 (2019).

29. European Food Safety Authority. Peer review of the pesticide risk assessment of the potential endocrine disrupting properties of glyphosate. *EFSA J.* **15**, (2017).

30. EC. Council Directive 98/83/EC of 3 November 1998 on the quality of water intended for human consumption. *Off. J. Eur. communities* **41**, 32–54 (1998).

31. Sawyer, C. N., McCarty, P. L. & Parkin, G. F. *Chemistry for environmental engineers*. (McGraw-Hill Education, 2002).

32. FAO and IWMI. *More people, more food, worse water? a global review of water pollution from agriculture*. (2018).

33. Hartmann, A., Lange, J., Weiler, M., Arbel, Y. & Greenbaum, N. A new approach to model the spatial and temporal variability of recharge to karst aquifers. *Hydrol. Earth Syst. Sci.* **16**, (2012).

34. Hartmann, A., Barberá, J. A., Lange, J., Andreo, B. & Weiler, M. Progress in the hydrologic simulation of time variant recharge areas of karst systems - Exemplified at a karst spring in Southern Spain. *Adv. Water Resour.* **54**, (2013).

35. Wada, Y., Wisser, D. & Bierkens, M. F. P. Global modeling of withdrawal, allocation and consumptive use of surface water and groundwater resources. *Earth Syst. Dyn.* **5**, 15–40 (2014).

36. Baldocchi, D. *et al.* FLUXNET: A New Tool to Study the Temporal and Spatial Variability of Ecosystem–Scale Carbon Dioxide, Water Vapor, and Energy Flux Densities. *Bull. Am. Meteorol. Soc.* **82**, 2415–2434 (2001).

37. Dorigo, W. A. *et al.* The International Soil Moisture Network: A data hosting facility for global in situ soil moisture measurements. *Hydrol. Earth Syst. Sci.* **15**, 1675–1698 (2011).

38. Mudarra, M., Hartmann, A. & Andreo, B. Combining Experimental Methods and Modeling to Quantify the Complex Recharge Behavior of Karst Aquifers. *Water Resour. Res.* 1–21 (2019). doi:10.1029/2017WR021819

39. Hartmann, A. *et al.* Model-aided quantification of dissolved carbon and nitrogen release after windthrow disturbance in an Austrian karst system. *Biogeosciences* **13**, (2016).

40. Allen, S. T. *et al.* Global sinusoidal seasonality in precipitation isotopes. *Hydrol. Earth Syst. Sci. Discuss.* 1–23 (2019). doi:10.5194/hess-2019-61

Acknowledgments

Support to Andreas Hartmann was provided by the Emmy Noether Programme of the German Research Foundation (DFG; grant no. HA 8113/1-1; project "Global Assessment of Water Stress in Karst Regions in a Changing World"). We thank Scott T. Allen (University of Utah) for his advice during the calculation of the Young Water Fractions of the carbonate rock springs.

Author contributions

Paper conceived by AH with input from SJ, TG, YW and TW. AH prepared and analysed the simulations with advice from SJ, TG, YW and TW. BA, JAB, HB, LB, JBC, WGD, MF, JG, NG, MK, HK, BL, JL, GL, JFM, MM, DS, CS, and EZ provided the water isotope observations to calculate the Young Water Fractions at the 119 carbonate rock springs and helped interpret the results. SJ provided support to AH when calculating and analysing the Young Water Fractions from the carbonate rock springs. All authors contributed to the writing of the manuscript.

Author Information

The authors declare no competing financial interests. Correspondence and requests for materials should be addressed to A.H. (andreas.hartmann@hydmod.uni-freiburg.de).

Data and materials availability

The code of the carbonate rock recharge model is available at https://github.com/KarstHub/VarKarst- R-2015. The raw data of the Glyphosate concentrations in groundwater is freely available at https://www.waterqualitydata.us. All data supporting the findings in this study are available within the paper and its supplementary information.

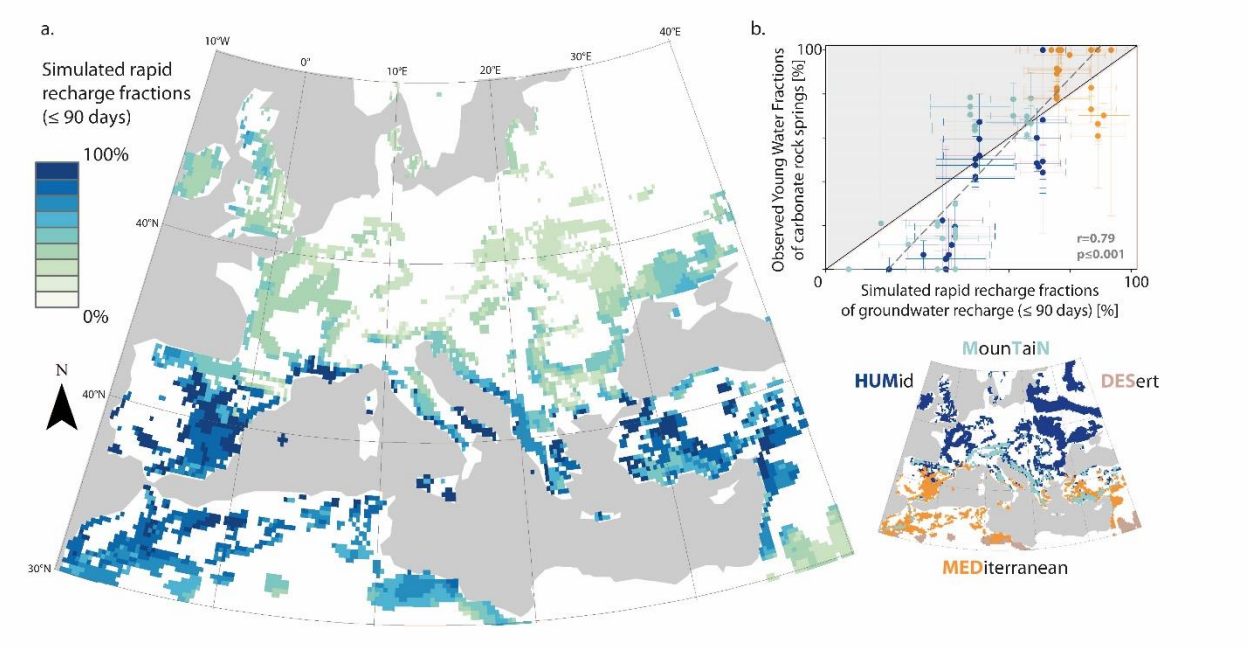

Fig. 1: The simulated rapid recharge fractions of groundwater recharge [%] across the study domain show the highest values of rapid recharge fractions in the Mediterranean. A comparison with observed Young Water Fractions of carbonate rock springs indicates realistic model behaviour. (a) Simulated rapid recharge fractions of groundwater recharge (≤ 90 days; same map with ≤ 60 days in Figure S3), (b) simulated rapid recharge fractions of groundwater recharge (≤ 90 days) compared to observed Young Water Fractions of the carbonate rock springs across the simulation domain (see methods in supplement); whiskers indicate standard error of simulations and observations.

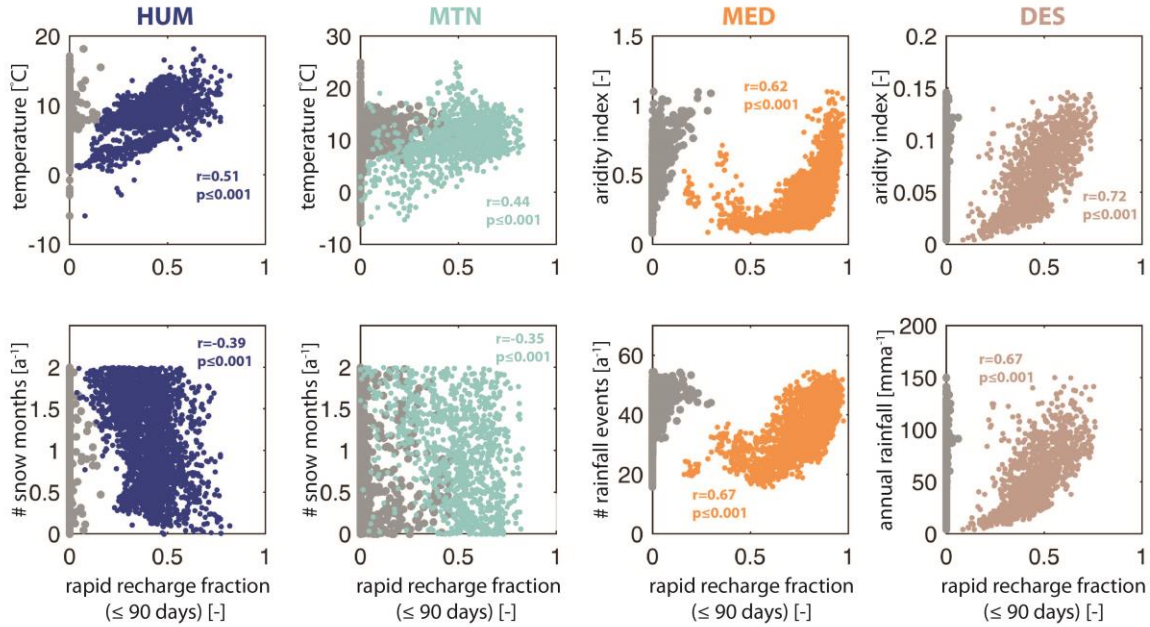

Fig. 2: Scatter plots of the strongest and 2nd strongest correlation of rapid recharge fractions (90-day threshold) and climatic descriptors for the humid (HUM), mountain (MTN), Mediterranean (MED), and desert (DES) regions. Aridity index, the average number of rainfall events and mean annual precipitation have the strongest control on rapid recharge fractions at the Mediterranean and the desert regions. Grey dots indicate the same relations but with rapid recharge fractions derived from the model with concentrated recharge not considered. The same figure including all investigated climate variables (60- and 90-day threshold) can be found in the supplement (Figs S4 – S6 and Tables S1 – S2).

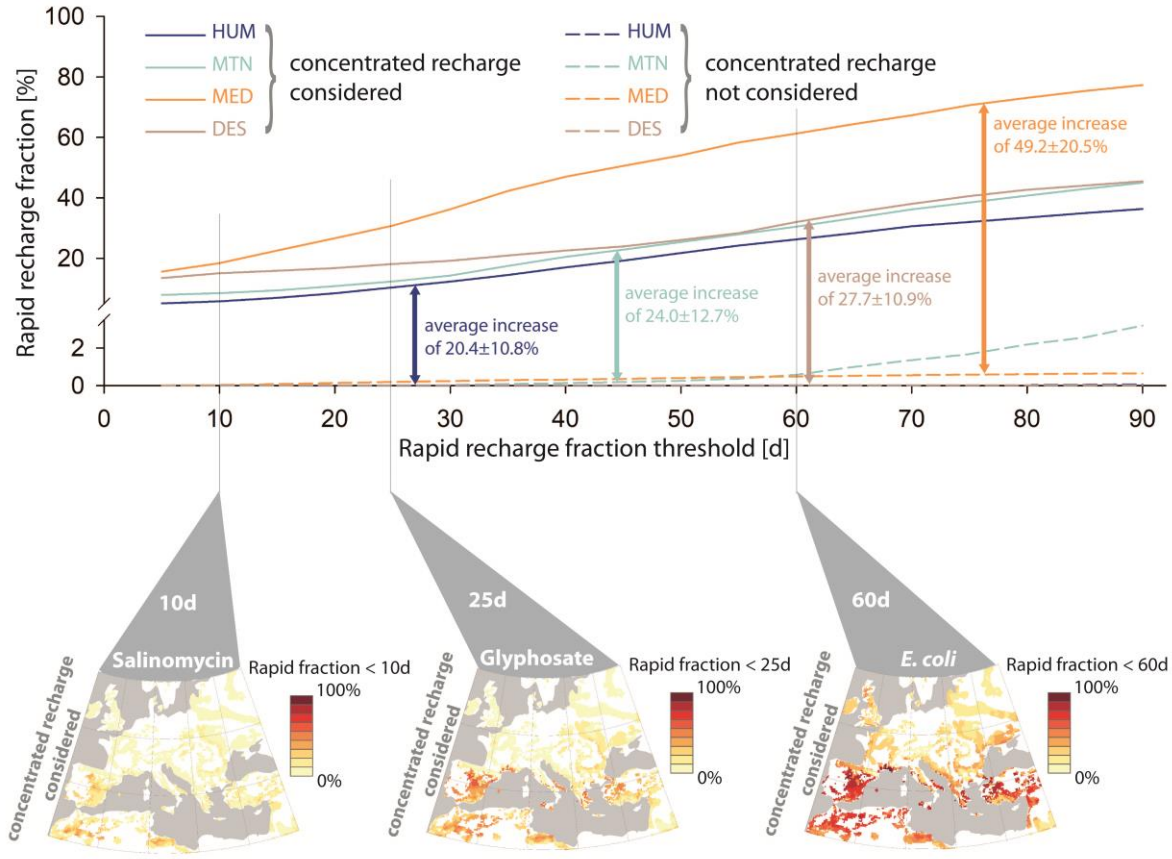

Fig. 3: Rapid recharge fractions of groundwater recharge for threshold times of 5 to 90 days for the four simulated regions and their spatial distribution for the three example pollutants. Solid lines represent the simulations including concentrated recharge processes while dashed lines indicate the rapid recharge fractions that would occur if concentrated recharge processes was not considered. The maps show the spatial distribution of rapid recharge fractions corresponding to the half-life times and survival times of Salinomycin, Glyphosate and *E. coli* when concentrated recharge is considered.

Supplemental material of manuscript entitled: Danger of groundwater contamination widely underestimated because of shortcuts for aquifer recharge

Submitted to: Nature Sustainability on April 23rd 2020

Authors: Andreas Hartmann[1,2*], Scott Jasechko[3], Tom Gleeson[4], Yoshihide Wada[5,6], Bartolomé Andreo[7], Juan Antonio Barberá[7], Heike Brielmann[8], Lhoussaine Bouchaou[9,10], Jean-Baptiste Charlier[11], W George Darling[12], Maria Filippini[13], Jakob Garvelmann[14,15], Nico Goldscheider[16], Martin Kralik[17], Harald Kunstmann[14,18], Bernard Ladouche[11], Jens Lange[19], Giorgia Lucianetti[20], José Francisco Martín[7], Matías Mudarra[7], Damián Sanchez[7], Christine Stumpp[21], Eleni Zagana[22], Thorsten Wagener[2,23]

Author affiliations:
[1] Chair of Hydrological Modeling and Water Resources, University of Freiburg, Germany
[2] Department of Civil Engineering, University of Bristol, United Kingdom
[3] Bren School of Environmental Science and Management, Univ. Calif. Santa Barbara, Santa Barbara, CA, 93117, USA
[4] Department of Civil Engineering and School of Earth and Ocean Sciences, University of Victoria, Canada
[5] International Institute for Applied Systems Analysis, Schlossplatz 1, A-2361, Laxenburg, Austria
[6] Department of Physical Geography, Utrecht University, Utrecht, The Netherlands, Heidelberglaan 2, 3584 CS Utrecht, The Netherlands
[7] Department of Geology and Centre of Hydrogeology at the University of Malaga (CEHIUMA), Malaga, Spain
[8] Austrian Federal Environmental Agency, Vienna, Austria
[9] Laboratory of Applied Geology and Geo- Environment, Ibn Zohr University, Agadir, Morocco
[10] Mohammed VI Polytechnic University, International Water Research Institute, Morocco
[11] BRGM, Univ. Montpellier, Montpellier, France
[12] British Geological Survey, Wallingford, United Kingdom
[13] Department of Biological Geological and Environmental Sciences, Alma Mater Studiorum - University of Bologna, Italy
[14] Institute of Meteorology and Climate Research, Karlsruhe Institute of Technology, Campus Alpin, Garmisch-Partenkirchen, Germany
[15] boden & grundwasser~ Allgäu GmbH, Sonthofen, Germany
[16] Institute of Applied Geosciences, Karlsruhe Institute of Technology (KIT), Karlsruhe, Germany
[17] Department of Environmental Geosciences, University of Vienna, Austria
[18] Institute of Geography, University of Augsburg, Augsburg, Germany
[19] Chair of Hydrology, University of Freiburg, Germany
[20] Department of Sciences, Roma Tre University, Largo S. Leonardo Murialdo 1, 00146 Rome, Italy
[21] University of Natural Resources and Life Sciences, Institute for Soil Physics and Rural Water Management, Muthgasse 18, 1190, Vienna, Austria
[22] Laboratory of Hydrogeology, Department of Geology, University of Patras, 26500 Rion Patras, Greece
[23] Cabot Institute, University of Bristol, United Kingdom

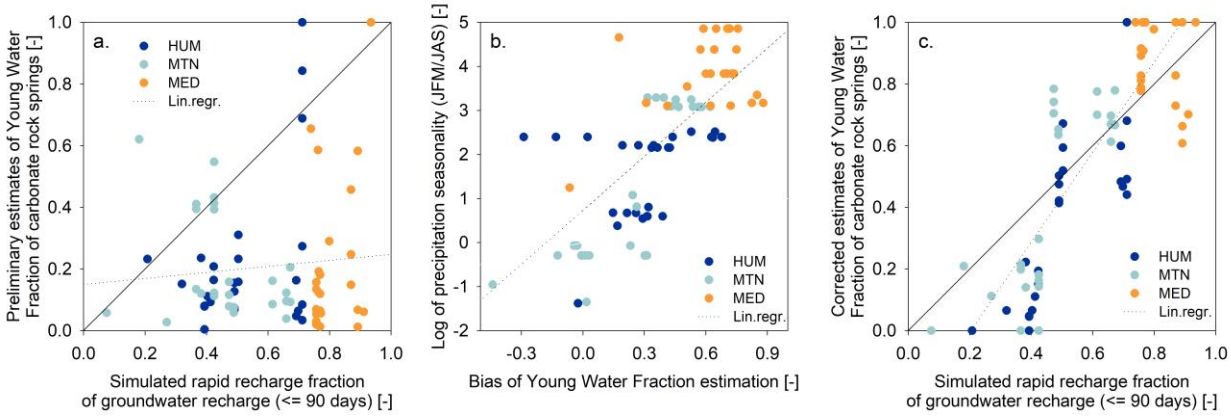

Fig. S 1.

Bias correction of Observed Young Water fractions of carbonate rock springs due to precipitation seasonality. (a) Relation between simulated rapid recharge fractions (90-day threshold) and preliminary estimates of Young Water Fractions of the carbonate rock springs ($r=0.09$, $p=0.46$), (b) relation between the bias of Young Water Fractions estimation defined as the difference between preliminary Young Water Fractions of the springs and the simulated rapid recharge fractions and the logarithm of rainfall seasonality defined as the sum of January, February and March precipitation divided by sum of July, August and September precipitation ($r=0.69$, $p\leq0.001$), and (c) relation between simulated rapid recharge fractions (90-day threshold) and precipitation seasonality corrected estimates of Young Water Fractions of the carbonate rock springs corrected by using the precipitation seasonality ($r=0.83$, $p\leq0.001$).

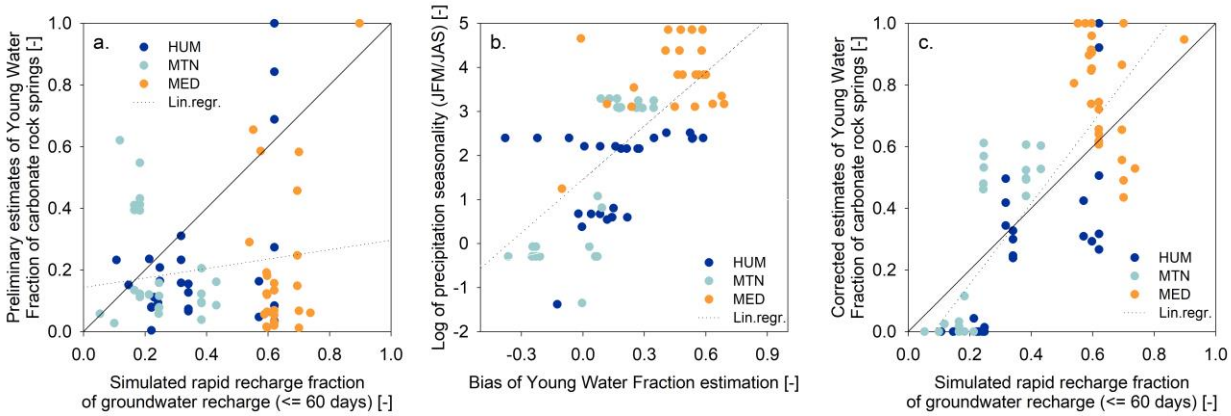

Fig. S 2.

Bias correction of Observed Young Water fractions of carbonate rock springs due to precipitation seasonality. (a) Relation between simulated rapid recharge fractions (60-day threshold) and preliminary estimates of Young Water Fractions of the carbonate rock springs ($r=0.14$, $p=0.21$), (b) relation between the bias of Young Water Fractions estimation defined as the difference between preliminary Young Water Fractions of the springs and the simulated rapid recharge fractions and the logarithm of rainfall seasonality defined as the sum of January, February and March precipitation divided by sum of July, August and September precipitation ($r=0.68$, $p\leq0.001$), and (c) relation between simulated rapid recharge fractions (60-day threshold) and precipitation seasonality corrected estimates of Young Water Fractions of the carbonate rock springs corrected by using the precipitation seasonality ($r=0.79$, $p\leq0.001$).

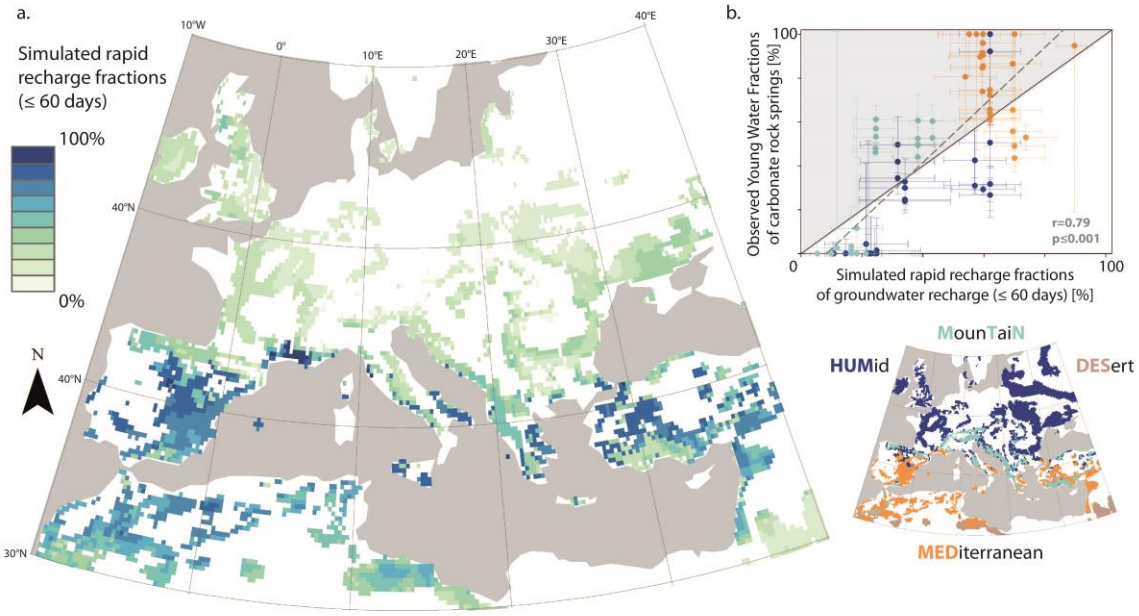

Fig. S 3.

The simulated rapid recharge fractions of groundwater recharge [%] across the study domain show the highest values of rapid recharge fractions in the Mediterranean. A comparison with observed Young Water Fractions of carbonate rock springs indicates realistic model behaviour. (a) Simulated rapid recharge fractions of groundwater recharge (≤ 60 days), (b) simulated rapid recharge fractions of groundwater recharge (≤ 60 days) compared to observed Young Water Fractions of the carbonate rock springs across the simulation domain (see methods); whiskers indicate standard error of simulations and observations.

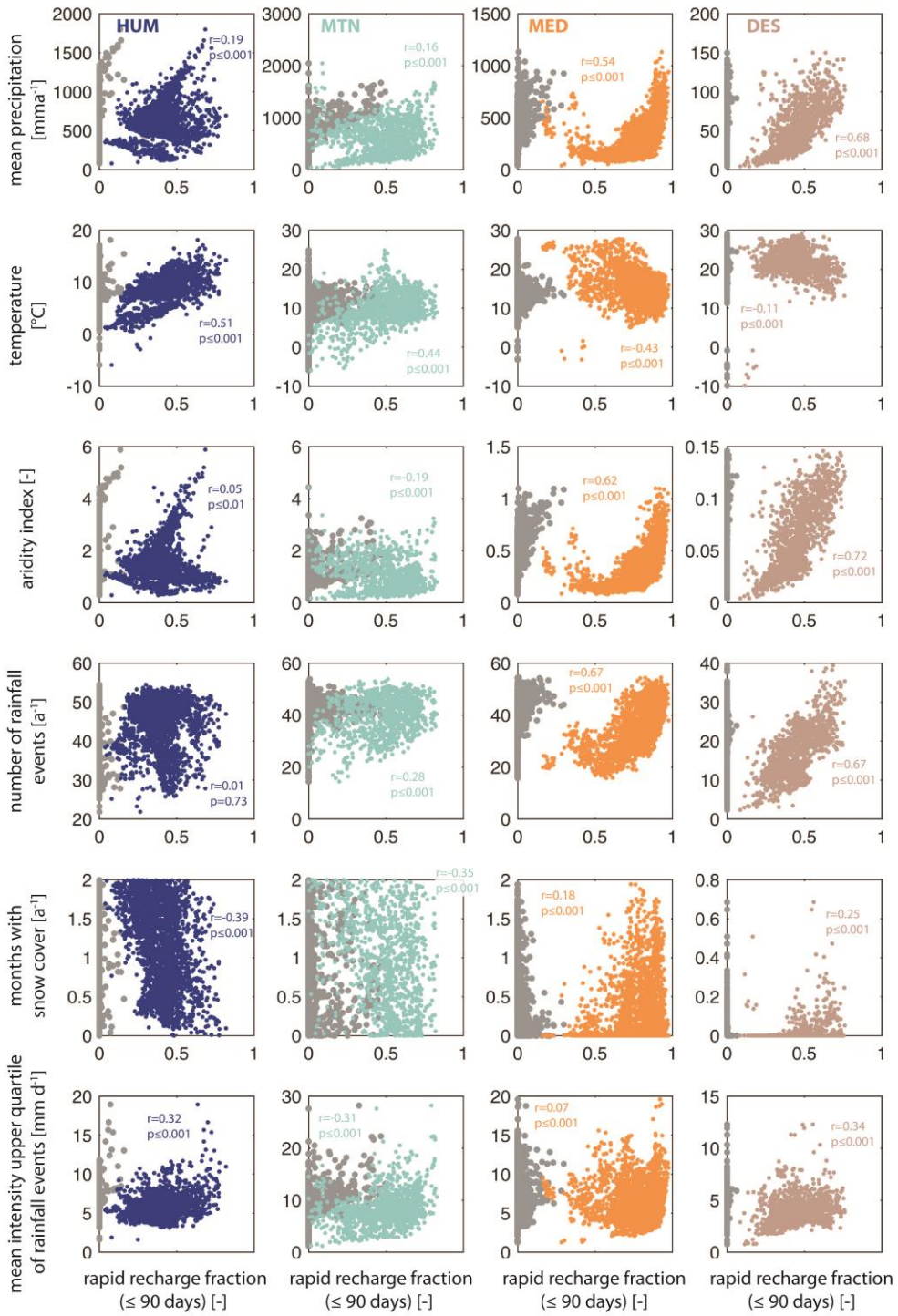

Fig. S 4.

Scatter plots showing how rapid recharge fractions (≤ 90 days) correlate with all climatic descriptors for the humid, mountain, Mediterranean and desert regions. Grey dots indicate the same relations but with rapid recharge fractions derived from the model with concentrated

recharge not considered.

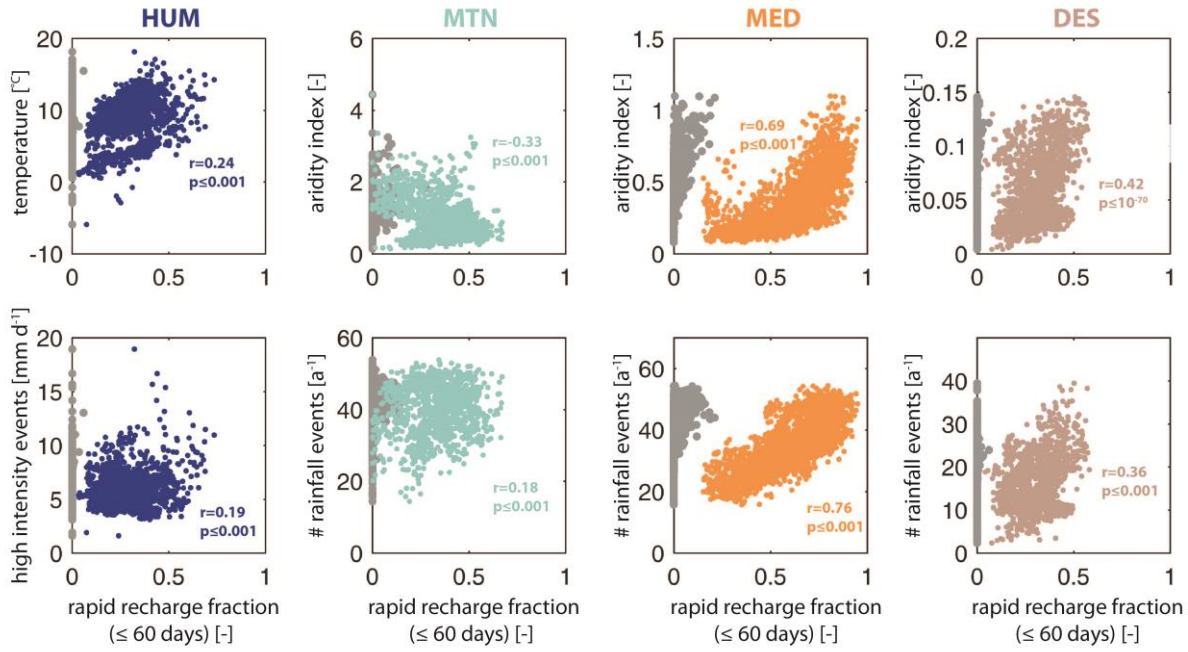

Fig. S 5.

Scatter plots of the strongest and 2nd strongest correlation of rapid recharge fractions (60-day threshold) and climatic descriptors for the humid (HUM), mountain (MTN), Mediterranean (MED), and desert (DES) regions. Aridity index, the average number of rainfall events and mean annual precipitation have the strongest control on rapid recharge fractions at the Mediterranean and the desert regions. Grey dots indicate the same relations but with rapid recharge fractions derived from the model with concentrated recharge not considered.

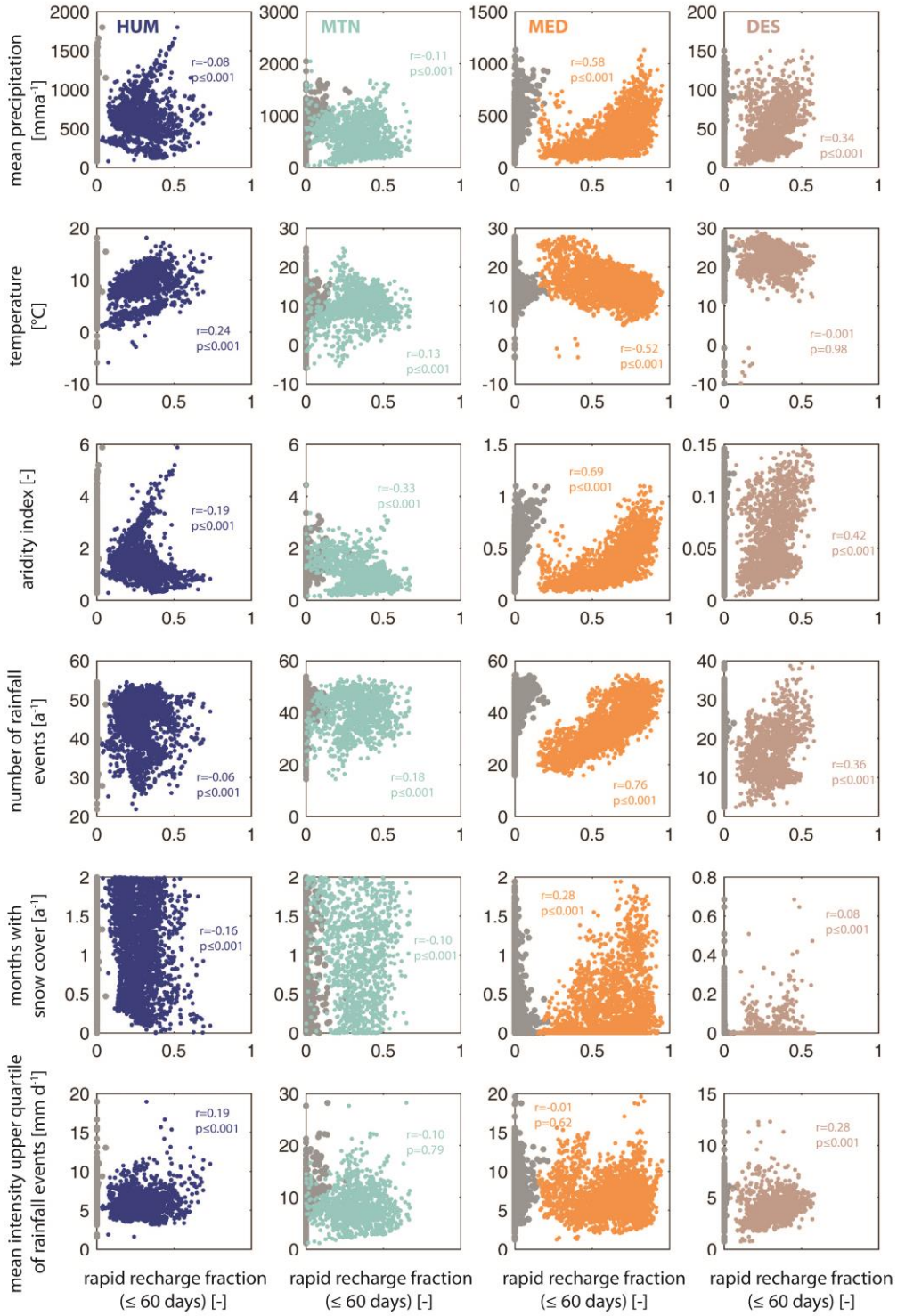

Fig. S 6.

Scatter plots showing how rapid recharge fractions (≤ 90 days) correlate with all climatic descriptors for the humid, mountain, Mediterranean and desert regions. Grey dots indicate the same relations but with rapid recharge fractions derived from the model with concentrated

recharge not considered.

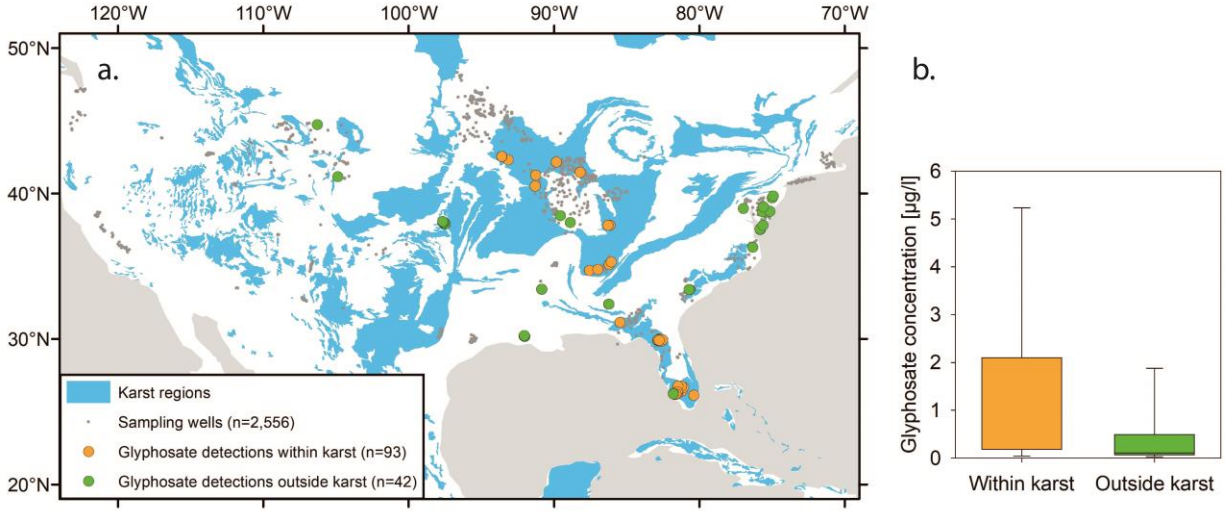

Fig. S 7.

Glyphosate was detected ~5.3 times more often within carbonate rock regions, and with concentrations ~4.1 times higher compared to non-carbonate rocks regions in a study across the contiguous United States[1,2]. (a) Location of sampling wells relative to the location of karst regions over the United States (derived from the World Karst Map[3]), Glyphosate detections within karst areas (93 out of 751) and Glyphosate detections outside karst areas (42 out of 1805), and (b) Concentrations among Glyphosate detections within and outside the karst. Whiskers indicate the 10th and 90th percentile; boxes and intermediate lines the 25th, 50th and 75th percentile.

Supplemental tables

Table S 1.

Correlation r_{YWF3} between simulated rapid recharge (≤ 90 days) and climatic descriptors, and the respective p-values for the four different carbonate rock landscapes. Strongest correlations are marked bold.

Variable Name	Unit	HUM		MTN		MED		DES	
		r_{YWF3}	p-value	r_{YWF3}	p-value	r_{YWF3}	p-value	r_{YWF3}	p-value
Precipitation	mm a^{-1}	0.19	≤0.001	0.16	≤0.001	0.54	≤0.001	**0.68**	**≤0.001**
Temperature	C°	**0.51**	**≤0.001**	**0.44**	**≤0.001**	-0.43	≤0.001	-0.11	≤0.001
Aridity Index	-	0.05	≤0.01	-0.19	≤0.001	**0.62**	**≤0.001**	**0.72**	**≤0.001**
# Rainfall events	-	0.01	0.73	0.28	≤0.001	**0.67**	**≤0.001**	0.67	≤0.001
# Snow cover	months a^{-1}	**-0.39**	**≤0.001**	**-0.35**	**≤0.001**	0.18	≤0.001	0.25	≤0.001
High intensity events	mm d^{-1}	0.32	≤0.001	0.31	≤0.001	0.07	≤0.001	0.34	≤0.001

Table S 2.

Correlation r_{YWF2} between simulated rapid recharge (≤ 60 days) and climatic descriptors, and the respective p-values for the four different carbonate rock landscapes. Strongest correlations are marked bold.

Variable Name	Unit	HUM		MTN		MED		DES	
		r_{YWF2}	p-value	r_{YWF2}	p-value	r_{YWF2}	p-value	r_{YWF2}	p-value
Precipitation	mm a^{-1}	-0.08	≤0.001	-0.11	≤0.001	0.58	≤0.001	0.34	≤0.001
Temperature	C°	**0.24**	**≤0.001**	0.13	≤0.001	-0.52	≤0.001	0.001	0.98
Aridity Index	-	-0.19	≤0.001	**-0.33**	**≤0.001**	**0.69**	**≤0.001**	**0.42**	**≤0.001**
# Rainfall events	a^{-1}	-0.06	≤0.001	**0.18**	**≤0.001**	**0.76**	**≤0.001**	**0.36**	**≤0.001**
# Snow cover	months a^{-1}	-0.16	≤0.001	-0.10	≤0.001	0.28	≤0.001	0.08	≤0.001
High intensity events	mm d^{-1}	**0.19**	**≤0.001**	-0.01	0.79	-0.01	0.62	0.28	≤0.001

Table S 3.

Observed Young Water Fractions of the precipitation seasonality corrected 78 remaining carbonate rock springs as well as simulated rapid recharge fractions of recharge for the 90-day threshold. The identifier includes the country code of each carbonate rock spring followed in the next column by the name of each spring. Coordinates are provided in latitude and longitude (WGS84), both Young Water Fractions and rapid recharge fractions are given in % (SE: standard error).

Identifier	Name	Latitude (WGS84)	Longitude (WGS84)	Corrected Young Water Fraction [%]	SE Young Water Fraction [%]	Rapid Recharge Fraction (90 days) [%]	SE Rapid Recharge Fraction (90 days) [%]
CH-0001	Rappenfluh	47.487	7.666	0.00	0.07	0.32	0.14
ES-0002	Benaojan (Spring S-2)	36.715	-5.245	0.82	0.10	0.66	0.13
ES-0004	Pileta	36.665	-5.280	1.00	0.63	0.89	0.09
ES-0005	Genal	36.640	-5.118	0.74	0.08	0.66	0.13
ES-0006	Verde	36.672	-5.026	0.79	0.06	0.66	0.13
ES-0007	Grande	36.722	-4.938	0.89	0.12	0.67	0.13
ES-0008	Jorox	36.732	-4.891	0.78	0.08	0.67	0.13
ES-0021	Canamero	36.893	-4.998	0.76	0.06	0.91	0.08
FR-0046	St. Andre	43.693	3.601	1.00	0.76	0.93	0.05
FR-0047	Rogues	43.879	3.600	1.00	0.65	0.71	0.07
FR-0048	Hortus	43.829	3.798	1.00	0.84	0.71	0.07
IL-0001	Dan	33.249	35.653	0.93	0.04	0.77	0.11
IL-0002	Banias	33.248	35.695	0.87	0.02	0.77	0.11
FR-0049-L	Fontanilles	43.753	3.623	0.52	0.08	0.71	0.07
FR-0050-L	Cents-Fonts	43.760	3.624	0.71	0.12	0.71	0.07
FR-0051-L	Bueges	43.813	3.591	0.47	0.07	0.71	0.07
FR-0052-L	Lamalou	43.823	3.801	1.00	0.33	0.71	0.07
ES-0001-L	9_Canos	36.681	-5.445	0.79	0.04	0.89	0.09
ES-0002-L	Algarrobal	36.671	-5.446	0.84	0.08	0.89	0.09
ES-0003-L	Arroyomolinos	36.810	-5.373	1.00	0.17	0.87	0.08
ES-0004-L	Benamahoma	36.768	-5.463	1.00	0.10	0.87	0.08
ES-0005-L	Bocaleones	36.768	-5.463	0.96	0.06	0.87	0.08
SL-0001-L	Timavo	45.786	13.587	0.40	0.07	0.50	0.12
SL-0002-L	Sardos	45.793	13.587	0.55	0.13	0.50	0.12
SL-0003-L	Moschenizze_North	45.803	13.582	0.47	0.09	0.50	0.12
GB-0001-L	Blewbury	51.567	-1.239	0.00	0.37	0.38	0.13
GB-0002-L	E_Ginge	51.577	-1.358	0.00	0.09	0.39	0.13

GB-0003-L	Jannaways	51.425	-1.355	0.00	0.16	0.42	0.13
GB-0004-L	Kimber	51.439	-1.164	0.00	0.12	0.41	0.13
GB-0005-L	Letcombe_B	51.565	-1.461	0.00	0.50	0.39	0.13
GB-0006-L	Upton	51.573	-1.253	0.00	0.51	0.39	0.13
GB-0007-L	Weston	51.463	-1.426	0.00	0.11	0.42	0.13
GB-0008-L	Woolstone	51.582	-1.574	0.00	0.17	0.40	0.13
AT-0002-L	Hammerbachquelle	47.210	15.350	0.00	0.05	0.21	0.12
AT-0004-L	Gerstenboedenquelle	47.260	9.770	0.03	0.03	0.27	0.10
JO-0001-L	Tanour Spring	32.408	35.745	1.00	0.19	0.74	0.12
FR-0001-A	Cernon	43.975	3.146	0.43	0.04	0.69	0.08
FR-0002-A	Durzon	43.991	3.262	0.47	0.02	0.70	0.07
FR-0003-A	Esperelle	44.121	3.208	0.04	0.05	0.49	0.13
FR-0004-A	Homede	44.077	3.060	0.04	0.05	0.49	0.13
FR-0005-A	Boundou	44.067	3.048	0.10	0.06	0.49	0.13
FR-0006-A	Lavencou	44.036	3.042	0.12	0.10	0.49	0.13
FR-0007-A	Mouline	43.992	3.094	0.55	0.14	0.69	0.08
IT-0001-A	Molinetto	46.008	12.473	0.00	0.04	0.42	0.11
IT-0002-A	Santissima	46.021	12.475	0.07	0.21	0.42	0.11
IT-0003-A	Gorgazzo	46.040	12.497	0.03	0.25	0.42	0.11
IT-0004-A	Agaroi	46.070	12.511	0.00	0.15	0.37	0.10
IT-0005-A	Budoia	46.076	12.512	0.21	0.20	0.37	0.10
IT-0006-A	Tornidor	46.073	12.511	0.23	0.13	0.37	0.10
IT-0007-A	Polla1 Santissima	46.018	12.476	0.05	0.71	0.42	0.11
IT-0008-A	Polla2 Santissima	46.018	12.476	0.19	0.32	0.42	0.11
IT-0009-A	Cavalli	46.010	12.477	0.00	0.08	0.42	0.11
IL-0001-A	Ein Moda	32.496	35.445	0.97	0.08	0.77	0.11
IL-0002-A	Ein Harod	32.548	35.355	1.00	0.13	0.76	0.10
IL-0003-A	Ein Homa & Ein Migdal	32.500	35.453	1.00	0.12	0.76	0.10
IL-0004-A	Ein Amall	32.505	35.445	0.93	0.07	0.76	0.10
IL-0005-A	Leshem	33.249	35.651	0.99	0.06	0.77	0.11
IL-0006-A	Kezinim	33.247	35.688	0.82	0.02	0.77	0.11
IQ-0001	Sarwchawa	36.280	44.757	0.90	0.02	0.76	0.11
IQ-0002	Shkarta	36.306	44.722	0.87	0.03	0.76	0.11
IQ-0003	Betwata	36.343	44.709	0.86	0.01	0.76	0.11
IQ-0004	Zewa	36.396	44.645	0.91	0.03	0.76	0.11
IQ-0005	Chewqa	36.349	44.578	0.87	0.04	0.76	0.11
IQ-0006	Bla	36.519	44.493	0.95	0.04	0.38	0.12
IQ-0007	Qala Saida	36.340	44.765	0.98	0.04	0.76	0.11
IQ-0008	Gullan	36.388	44.694	1.00	0.05	0.76	0.11
LB-0001	Jeita	33.944	35.642	0.90	0.04	0.47	0.13

LB-0002	Naber al Labbane	33.995	35.828	0.86	0.03	0.47	0.13
LB-0003	Naber al Assal	34.010	35.839	0.87	0.02	0.49	0.14
LB-0004	Kashkoush	33.943	35.639	0.94	0.06	0.47	0.13
LB-0005	Afqa	34.068	35.893	0.85	0.02	0.49	0.14
LB-0006	Rouaiss	34.109	35.909	0.87	0.03	0.49	0.14
PA-0001	Sultan_Elisha	31.870	35.443	1.00	0.53	0.76	0.13
GR-0001	Uni Patras P1	37.868	22.473	0.67	0.04	0.61	0.07
GR-0002	Uni Patras P2	37.869	22.464	0.74	0.07	0.61	0.07
IT-0001	Angheraz spring	46.284	11.922	0.25	0.06	0.07	0.05
IT-0002	Pradidali spring	46.228	11.869	0.53	0.99	0.18	0.09
MA-0001	WT spring	30.681	-9.345	1.00	0.25	0.80	0.12

Table S 4.

Observed Young Water Fractions of the precipitation seasonality corrected 78 remaining carbonate rock springs as well as simulated rapid recharge fractions of recharge for the 60-day threshold. The identifier includes the country code of each carbonate rock spring followed in the next column by the name of each spring. Coordinates are provided in latitude and longitude (WGS84), both Young Water Fractions and rapid recharge fractions are given in % (SE: standard error).

Identifier	Name	Latitude (WGS84)	Longitude (WGS84)	Corrected Young Water Fraction [%]	SE Young Water Fraction [%]	Rapid Recharge Fraction (60 days) [%]	SE Rapid Recharge Fraction (60 days) [%]
CH-0001	Rappenfluh	47.487	7.666	0.00	0.07	0.15	0.12
ES-0002	Benaojan (Spring S-2)	36.715	-5.245	0.64	0.10	0.38	0.08
ES-0004	Pileta	36.665	-5.280	1.00	0.63	0.70	0.10
ES-0005	Genal	36.640	-5.118	0.56	0.08	0.38	0.08
ES-0006	Verde	36.672	-5.026	0.62	0.06	0.38	0.08
ES-0007	Grande	36.722	-4.938	0.72	0.12	0.38	0.08
ES-0008	Jorox	36.732	-4.891	0.61	0.08	0.38	0.08
ES-0021	Canamero	36.893	-4.998	0.58	0.06	0.74	0.10
FR-0046	St. Andre	43.693	3.601	1.00	0.76	0.90	0.06
FR-0047	Rogues	43.879	3.600	1.00	0.65	0.62	0.10
FR-0048	Hortus	43.829	3.798	1.00	0.84	0.62	0.10
IL-0001	Dan	33.249	35.653	0.75	0.04	0.60	0.10
IL-0002	Banias	33.248	35.695	0.70	0.02	0.60	0.10
FR-0049-L	Fontanilles	43.753	3.623	0.34	0.08	0.62	0.10
FR-0050-L	Cents-Fonts	43.760	3.624	0.53	0.12	0.62	0.10
FR-0051-L	Bueges	43.813	3.591	0.29	0.07	0.62	0.10
FR-0052-L	Lamalou	43.823	3.801	0.95	0.33	0.62	0.10
ES-0001-L	9_Canos	36.681	-5.445	0.61	0.04	0.70	0.10
ES-0002-L	Algarrobal	36.671	-5.446	0.66	0.08	0.70	0.10
ES-0003-L	Arroyomolinos	36.810	-5.373	1.00	0.17	0.70	0.09
ES-0004-L	Benamahoma	36.768	-5.463	0.88	0.10	0.70	0.09
ES-0005-L	Bocaleones	36.768	-5.463	0.78	0.06	0.70	0.09
SL-0001-L	Timavo	45.786	13.587	0.22	0.07	0.32	0.12
SL-0002-L	Sardos	45.793	13.587	0.38	0.13	0.32	0.12
SL-0003-L	Moschenizze_North	45.803	13.582	0.30	0.09	0.32	0.12
GB-0001-L	Blewbury	51.567	-1.239	0.00	0.37	0.21	0.14
GB-0002-L	E_Ginge	51.577	-1.358	0.00	0.09	0.22	0.14

GB-0003-L	Jannaways	51.425	-1.355	0.00	0.16	0.25	0.14
GB-0004-L	Kimber	51.439	-1.164	0.00	0.12	0.24	0.14
GB-0005-L	Letcombe_B	51.565	-1.461	0.00	0.50	0.22	0.14
GB-0006-L	Upton	51.573	-1.253	0.00	0.51	0.22	0.14
GB-0007-L	Weston	51.463	-1.426	0.00	0.11	0.25	0.14
GB-0008-L	Woolstone	51.582	-1.574	0.00	0.17	0.23	0.15
AT-0002-L	Hammerbachquelle	47.210	15.350	0.00	0.05	0.11	0.11
AT-0004-L	Gerstenboedenquelle	47.260	9.770	0.00	0.03	0.10	0.04
JO-0001-L	Tanour Spring	32.408	35.745	1.00	0.19	0.55	0.10
FR-0001-A	Cernon	43.975	3.146	0.26	0.04	0.57	0.10
FR-0002-A	Durzon	43.991	3.262	0.30	0.02	0.60	0.10
FR-0003-A	Esperelle	44.121	3.208	0.00	0.05	0.34	0.15
FR-0004-A	Homede	44.077	3.060	0.00	0.05	0.34	0.15
FR-0005-A	Boundou	44.067	3.048	0.00	0.06	0.34	0.15
FR-0006-A	Lavencou	44.036	3.042	0.00	0.10	0.34	0.15
FR-0007-A	Mouline	43.992	3.094	0.37	0.14	0.57	0.10
IT-0001-A	Molinetto	46.008	12.473	0.00	0.04	0.18	0.08
IT-0002-A	Santissima	46.021	12.475	0.00	0.21	0.18	0.08
IT-0003-A	Gorgazzo	46.040	12.497	0.00	0.25	0.18	0.08
IT-0004-A	Agaroi	46.070	12.511	0.00	0.15	0.17	0.08
IT-0005-A	Budoia	46.076	12.512	0.04	0.20	0.17	0.08
IT-0006-A	Tornidor	46.073	12.511	0.05	0.13	0.17	0.08
IT-0007-A	Polla1 Santissima	46.018	12.476	0.00	0.71	0.18	0.08
IT-0008-A	Polla2 Santissima	46.018	12.476	0.02	0.32	0.18	0.08
IT-0009-A	Cavalli	46.010	12.477	0.00	0.08	0.18	0.08
IL-0001-A	Ein Moda	32.496	35.445	0.79	0.08	0.59	0.10
IL-0002-A	Ein Harod	32.548	35.355	0.92	0.13	0.60	0.11
IL-0003-A	Ein Homa & Ein Migdal	32.500	35.453	0.86	0.12	0.60	0.11
IL-0004-A	Ein Amall	32.505	35.445	0.75	0.07	0.60	0.11
IL-0005-A	Leshem	33.249	35.651	0.81	0.06	0.60	0.10
IL-0006-A	Kezinim	33.247	35.688	0.64	0.02	0.60	0.10
IQ-0001	Sarwchawa	36.280	44.757	0.72	0.02	0.62	0.10
IQ-0002	Shkarta	36.306	44.722	0.69	0.03	0.62	0.10
IQ-0003	Betwata	36.343	44.709	0.69	0.01	0.62	0.10
IQ-0004	Zewa	36.396	44.645	0.73	0.03	0.62	0.10
IQ-0005	Chewqa	36.349	44.578	0.70	0.04	0.62	0.10
IQ-0006	Bla	36.519	44.493	0.77	0.04	0.21	0.08
IQ-0007	Qala Saida	36.340	44.765	0.80	0.04	0.62	0.10
IQ-0008	Gullan	36.388	44.694	0.82	0.05	0.62	0.10
LB-0001	Jeita	33.944	35.642	0.72	0.04	0.25	0.07

LB-0002	Naber al Labbane	33.995	35.828	0.69	0.03	0.25	0.07
LB-0003	Naber al Assal	34.010	35.839	0.69	0.02	0.24	0.08
LB-0004	Kashkoush	33.943	35.639	0.77	0.06	0.25	0.07
LB-0005	Afqa	34.068	35.893	0.68	0.02	0.24	0.08
LB-0006	Rouaiss	34.109	35.909	0.69	0.03	0.24	0.08
PA-0001	Sultan_Elisha	31.870	35.443	1.00	0.53	0.58	0.11
GR-0001	Uni Patras P1	37.868	22.473	0.49	0.04	0.43	0.08
GR-0002	Uni Patras P2	37.869	22.464	0.57	0.07	0.43	0.08
IT-0001	Angheraz spring	46.284	11.922	0.07	0.06	0.05	0.04
IT-0002	Pradidali spring	46.228	11.869	0.36	0.99	0.12	0.08
MA-0001	WT spring	30.681	-9.345	1.00	0.25	0.54	0.10

References

1. Scribner, E. A., Battaglin, W. A., Gilliom, R. J. & Meyer, M. T. Concentrations of Glyphosate, Its Degradation Product, Aminomethylphosphonic Acid, and Glufosinate in Ground- and Surface-Water, Rainfall, and Soil Samples Collected in the United States, 2001–06. *U.S. Geol. Surv. Sci. Investig. Rep.* **2007**–**5122**, (2007).

2. Read, E. K. *et al.* Water quality data for national-scale aquatic research: The Water Quality Portal. *Water Resour. Res.* **53**, 1735–1745 (2017).

3. Chen, Z. *et al.* The World Karst Aquifer Mapping project: concept, mapping procedure and map of Europe. *Hydrogeol. J.* (2017). doi:10.1007/s10040-016-1519-3